

1 **Activation of the chicken type I IFN response by infectious bronchitis coronavirus.**

2

3 Joeri Kint^{1,2}, Marcela Fernandez-Gutierrez¹, Helena J. Maier³, Paul Britton³, Martijn A. Langereis⁴,
4 Joseph Koumans², Geert F Wiegertjes¹, Maria Forlenza^{1,#}

5

6 ¹Cell Biology and Immunology Group, Wageningen Institute of Animal Sciences, Wageningen
7 University, Wageningen, The Netherlands.

8 ²MSD Animal Health, Bioprocess Technology & Support, Boxmeer, The Netherlands

9 ³Avian Viral Diseases, The Pirbright Institute, Compton Laboratory, United Kingdom.

10 ⁴Department of Infectious Diseases and Immunology, Faculty of Veterinary Medicine, Utrecht
11 University, Utrecht, The Netherlands

12

13 # Correspondence should be addressed to M.F. (maria.forlenza@wur.nl)

14

15 **Abstract**

16 Coronaviruses from both the *Alpha* and *Betacoronavirus* genera, interfere with the type I interferon
17 (IFN) response in various ways, ensuring limited activation of the IFN response in most cell types.

18 Of *Gammacoronaviruses* that mainly infect birds, little is known about activation of the host
19 immune response. We show that the prototypical *Gammacoronavirus*, infectious bronchitis virus
20 (IBV), induces a delayed activation of the IFN response in primary renal cells, tracheal epithelial
21 cells and in a chicken cell line. *Ifnβ* expression in fact, is delayed with respect to the peak of viral
22 replication and accompanying accumulation of dsRNA. In addition, we demonstrate that MDA5 is
23 the primary sensor for *Gammacoronavirus* infections in chicken cells. Furthermore, we provide
24 evidence that accessory proteins 3a and 3b of IBV modulate the IFN response at the transcriptional
25 and translational level. Finally, we show that, despite the lack of activation of the IFN response
26 during the early phase of IBV infection, signalling of non-self dsRNA through both MDA5 and TLR3
27 remains intact in IBV-infected cells. Taken together, this study provides the first comprehensive
28 analysis of host-virus interactions of a *Gammacoronavirus* with avian innate immune responses.

29

30 **Importance:** Our results demonstrate that IBV has evolved multiple strategies to avoid activation
31 of the type I interferon response. Taken together, the present study closes a gap in the
32 understanding of host-IBV interaction, and paves the way for further characterization of the
33 mechanisms underlying immune evasion strategies as well as pathogenesis of
34 *Gammacoronaviruses*.

35

36 **word count abstract: 198**

37

38 **Key words for referees:** Infectious bronchitis coronavirus; chicken; *Gammacoronavirus*; avian;
39 DF-1; CEK; type I IFN response; Ifn β ; MDA5; TLR3; RIG-I; RNA silencing; accessory proteins; 3b;
40 3a; RNA FISH

41

42

43

44

45 **Introduction**

46 Coronaviruses constitute a large family of positive-stranded RNA viruses and cause a range of
47 human and veterinary diseases. Infectious bronchitis virus (IBV) is the prototype avian coronavirus
48 from the *Gammacoronavirus* genus and the causative agent of a highly contagious respiratory
49 disease of major economic importance to the poultry industry (1). IBV enters the avian host
50 through the respiratory tract, where it causes destruction of the epithelium leading to respiratory
51 distress and initiation of secondary bacterial infections. Depending on the strain, IBV can also
52 spread to other epithelial surfaces such as the gastrointestinal tract, the kidneys and the oviduct,
53 the latter causing problems in egg production and quality (1-6). Contrary to coronaviruses from the
54 *Alpha* and *Beta* genera, including human coronavirus HCoV-229E, Severe Acute Respiratory
55 Syndrome (SARS-CoV), Middle East Respiratory Syndrome (MERS-CoV) and mouse hepatitis virus
56 (MHV), very little is known about how *Gammacoronaviruses* including IBV evade or interfere with
57 innate immune responses of their host.

58 Innate immune responses consist of a network of antimicrobial mechanisms, of which the type I
59 interferon (IFN) response is an essential defence mechanism against viruses. Typically, the type I
60 IFN response, from hereafter referred to as IFN response, is initiated upon activation of host
61 pattern recognition receptors (PRRs), present in all animal cells. Two families of PRRs have been
62 shown to be involved in the recognition of RNA viruses namely the membrane-bound Toll-like
63 receptors (TLRs) and the cytosolic RIG-I-like receptors (RLRs) (7). The primary ligands for
64 activation of these PRRs are double-stranded RNA (dsRNA) and 5' triphosphate-containing RNA,
65 normally absent from uninfected host-cells. Activation of RLRs leads to the transcription of genes
66 encoding type I interferons (IFN α and IFN β). These interferons are secreted from the infected cell
67 providing a signal for the infected as well as the neighbouring cells that induce the transcription of
68 anti-viral effector genes collectively called interferon stimulated genes (ISGs).

69 The ability of a virus to replicate and produce infectious progeny depends for a large part on its
70 ability to avoid induction or counteract the IFN response of its host. Indeed, a common feature of
71 *Alpha-* and *Betacoronaviruses*, including HCoV-229E, SARS-CoV, and MHV, is their limited
72 activation of the IFN response (8-13). This limited activation can be partially explained by
73 intracellular membrane rearrangements that might shield dsRNA and other viral components from
74 recognition by host PRRs (14, 15). In addition, coronavirus nsp16 displays 2'-O-methylase activity,
75 which results in 2'-O-methylation of a ribose moiety on the 5' cap of coronavirus mRNAs, making
76 them indistinguishable from host mRNAs (16). Furthermore, many other coronavirus proteins, such
77 as nsp1, nsp3, the nucleocapsid and many of the accessory proteins have been shown to interfere
78 with the IFN response in various ways (reviewed in (17, 18)).

79

80 Interaction between *Gammacoronaviruses* and innate immune responses of their avian hosts is
81 poorly understood. Early studies on *Gammacoronaviruses* in chicken suggest that IBV-induced IFN
82 production is variable and dependent on both virus strain and cell type. (19-22). Further, two
83 transcriptional studies on tissues collected after *in vivo* and *in ovo* IBV infections, found only limited
84 upregulation of ISGs at 1 - 3 days post-infection (23-25). Functional studies using IBV Beaudette
85 showed that it induced cell-cycle arrest and apoptosis (26, 27), that IBV interacts with eIF3f (28)
86 and that IBV inhibits protein kinase R activation, thereby maintaining protein synthesis (29).
87 Although these studies did provide a number of details on the interactions between IBV and the
88 host cell, most experiments were carried out in Vero cells. This non-avian cell line is one of the
89 very few cell lines in which the IBV-Beaudette strain has been adapted to grow, facilitating *in vitro*
90 experiments. Vero cells, however, lack the *Ifnβ* gene, preventing them from mounting a type I IFN
91 response (30, 31), reducing the value of Vero cells for research on innate immune responses to
92 IBV. In addition, the Beaudette strain is non-pathogenic *in vivo* with limited replication in host
93 tissues (32), reducing the value of these *in vitro* studies for translation to *in vivo* situations. For
94 these reasons, we used pathogenic isolates of IBV to infect primary chicken cells, and a chicken cell
95 line, as these isolates are known to infect, spread and cause clinical disease *in vivo*.

96

97 In the current study, we show that IBV infection leads to a significant induction of *Ifnβ* transcription
98 through an MDA5-dependent activation of the IFN response, albeit delayed with respect to both
99 virus replication and accumulation of dsRNA. This delayed induction of *Ifnβ* was further confirmed
100 through RNA FISH analysis showing that accumulation of *Ifnβ* mRNA is restricted to IBV-infected

101 and not neighbouring uninfected cells. Although the time lag between accumulation of dsRNA and
102 induction of *Ifn β* transcription might suggest that IBV interferes with recognition of dsRNA, we
103 observed that sensing of exogenous (non-self) dsRNA remained functional in IBV-infected cells.
104 Using mutant IBV viruses we demonstrate that both accessory proteins 3a and 3b are involved in
105 limiting *Ifn β* expression, as both 3a and 3b null viruses induced increased *Ifn β* expression.
106 Nevertheless, 3a and 3b seem to have a differential effect on IFN protein production, infection with
107 3a null virus induced lower IFN levels whereas a 3b null virus increased IFN production compared
108 to the parental virus. Altogether, our data suggest that IBV delays but does not prevent detection
109 by MDA5, and that accessory proteins 3a and 3b modulate the IFN response in avian cells. This is
110 the first study addressing immune evasion and interference strategies of IBV in chicken and not in
111 mammalian cells, providing information essential to further understanding of the pathogenesis of
112 *Gammacoronaviruses*.

113

114 **MATERIALS AND METHODS**

115 **Cells**

116 Chicken embryonic kidneys were aseptically removed from 17- to 19-day-old chicken embryo's
117 (Charles River, SPAFAS). A cell suspension was obtained by trypsinisation for 30 min at 37°C and
118 filtered through a 100 μ m mesh. The resulting chicken embryo kidney (CEK) cells were seeded at 4
119 $\times 10^5$ cells/cm² in 199 medium (Invitrogen) supplemented with 0.5% fetal bovine serum (FBS,
120 FASC) and 1% PenStrep (Gibco®, Invitrogen). Chicken trachea cells were isolated from 8- to 10-
121 week-old chickens (white leghorn). Tracheas were collected in ice-cold PBS, washed and stripped
122 from adipose tissue. Trachea were filled with a solution of 3.5 U/ml protease type XIV (Sigma), 4
123 U/ml DNase I (Qiagen) and 1% PenStrep in EMEM, sealed with clamps, and incubated overnight at
124 4°C. The next day, cells lining the luminal side of the trachea were flushed out with cold EMEM,
125 filtered through a cell strainer and seeded at 4 $\times 10^5$ cells/cm² in DMEM supplemented with 10%
126 FBS and 1% PenStrep. The RIG-I^{wt}, RIG-I^{KO}, MDA5^{wt} and MDA5^{KO} MEFs were provided by Prof. S.
127 Akira (33). The MAVS^{wt} and MAVS^{KO} MEFs were provided by Z.J. Chen (34). DF-1, CEC-32 and
128 MEFs cells were cultured in DMEM (Gibco®, Invitrogen) supplemented with 10% FBS and 1%
129 PenStrep. All cells were incubated in a humidified incubator at 37°C and 5% CO₂.

130

131

132 **DF-1 Ifn β -luc reporter cell line**

133 DF-1 cells were transfected using Fugene (Promega) according to the manufacturer's instructions
134 with a construct expressing firefly luciferase under the control of the -110bp proximal region of the
135 human *IFN β* promoter (35). Stably expressing cells were selected over a period of 3 weeks using
136 geneticin (500 μ g/ml). DF-1 Ifn β -luc stable cells were cultured in DMEM supplemented with 10%
137 FBS and 1% PenStrep and were not further subcloned.

138

139 **Viruses**

140 IBV-M41, IBV-QX and IBV-Italy-O2, Rift Valley Fever Virus clone 13 (RVFV CI13) and Infectious
141 Pancreatic Necrosis Virus (IPNV) were obtained from Merck Animal Health, Boxmeer, The
142 Netherlands. Sindbis-GFP was a kind gift from J. Fros, (Laboratory of Virology, Wageningen
143 University). IBV Beaudette, strain Beau-R, as well as the generation of the ScaUG3a, ScaUG3b,
144 ScaUG3ab and ScaUG5ab Beau-R null viruses has been published previously (36-38). In these
145 mutant IBV viruses, the start codons of the indicated accessory genes were mutated to stop
146 codons. All IBV strains were amplified and titrated on CEK cells. Sindbis-GFP was amplified on baby
147 hamster kidney (BHK) cells and titrated on CEK cells. RVFV CI13 was amplified and titrated on Vero
148 cells, an African green monkey cell line. IPNV was amplified and titrated on the CHSE-214,
149 Chinook-salmon cell line. IPNV was inactivated by 20 min UV exposure on a 48W BXT-26-M
150 (Uvitec).

151

152 **Poly I:C stimulation and RNase treatment**

153 Polyinosinic-poly(C) [p(I:C)] sodium was purchased from Sigma, dissolved in nuclease-free water
154 and stored at -80°C. p(I:C) was either directly added to the medium or transfected using
155 Lipofectamine 2000 (Invitrogen) as per manufacturer's instructions. DF-1 cells (3×10^5 /well) were
156 cultured in 24 well plates and transfected with 500 ng p(I:C). RNase treatment of CEK cell culture
157 supernatant was performed by addition of 10 μ g/ml RNase A (Invitrogen) before IBV infection or
158 before stimulation with 2 μ g/ml p(I:C).

159

160 **RNA isolation and cDNA synthesis**

161 Approximately 8×10^5 CEK cells or 3×10^5 DF-1 cells were lysed in RLT buffer (Qiagen) at various
162 time points after treatment or infection. RLT cell lysis buffer was spiked with 1 ng/sample of
163 luciferase mRNA (Promega) immediately prior to RNA isolation. Luciferase expression will later be

164 used as external reference gene for normalization during the gene expression analysis. Total RNA
165 was isolated using the RNeasy Mini Kit (Qiagen) according to the manufacturer's instructions,
166 including an on-column DNase treatment with RNase-free DNase (Qiagen). Before cDNA synthesis
167 of 0.5–1 µg total RNA, a second DNase treatment was performed using DNase I, amplification
168 grade (Invitrogen). Synthesis of cDNA was performed using SuperScript III (Invitrogen) using
169 random primers. cDNA samples were further diluted 1:50 in nuclease-free water before real-time
170 quantitative PCR analysis.

171

172 **Gene expression analysis**

173 Real-time quantitative PCR was performed on a Rotor-Gene 6000 (Corbett Research), using
174 Brilliant SYBR Green quantitative PCR (Stratagene) and primers (39-42) as listed in Table 1. Cycle
175 thresholds and amplification efficiencies were calculated by the Rotor-Gene software (version 1.7).
176 The relative expression ratio of the target gene was calculated using the average reaction efficiency
177 for each primer set and the cycle threshold (C_t) deviation of sample vs. control at time point 0h, as
178 described in (43). For calculation of the fold change of IBV total RNA, C_t deviation was calculated
179 versus C_t 30, as no IBV was present in the non-infected cells that were used as control in all the
180 experiments. Because expression of various housekeeping genes was unstable during virus
181 infections at time points later than 24 hours (data not shown), gene-expression ratios were
182 normalised using an external reference gene (luciferase).

183

184 **Immunohistochemistry**

185 CEK cells were seeded on fibronectin-coated glass Biocoat coverslips (BD Biosciences) at a density
186 of 1×10^5 cells/cm². After incubation at 37°C for 48 hours, cells were infected with IBV strain M41
187 at an MOI of 1, and fixed at different time points with 3.7% paraformaldehyde and permeabilized
188 using 0.1% Triton X-100. Infected cells were probed with anti-dsRNA antibody (English & Scientific
189 Consulting) and polyclonal chicken serum raised against IBV M41 was obtained from Merck AH.
190 Detection was done performed using Alexa 488 goat anti-mouse antibody (Invitrogen) and FITC
191 labelled goat anti-chicken antibody (Kirkegaard and Perry laboratories). Nuclei were stained with
192 4',6-diamidino-2-phenylindole (DAPI). Cells were imaged using a Zeiss Primo Vert microscope and
193 Axiovision software. Image overlays were made in ImageJ.

194

195 **RNA fluorescence *in situ* hybridization**

196 RNA fluorescence *in situ* hybridization (FISH) was performed according to previously described
197 protocols (44-46). A set of forty RNA FISH probes (20 bp), each labelled with one CAL Fluor® Red
198 610 fluorophore and targeting chicken *Ifnβ* (ENSGALT39477), was designed using the Stellaris®
199 probe designer (Biosearch Technologies; <https://www.biosearchtech.com/stellarisdesigner/>). The
200 coding sequence of chicken *Ifnβ* is 601 bp, therefore to accommodate the optimum number of
201 fluorescent probes (48, as explained in reference (44)), the 3'UTR was included in the probe design
202 tool. CEK cells were grown on fibronectin-coated coverslips (BD Biosciences) at a density of 2×10^5
203 cells/cm². After incubation at 37°C for 48 hours, cells were infected with IBV M41, and at the
204 indicated time points fixed in 70% ethanol at 4 °C. Hybridisation of the probes was performed
205 using the manufacturer's protocol for adherent cells. Imaging was performed using a Roper (Evry,
206 France) Spinning Disc Confocal System on a Nikon Eclipse Ti microscope using a 100 × Plan apo oil
207 immersion objective (NA 1.4) and a 491 nm laser line. Z-stacks were collected with 0.25 μm Z-
208 intervals. For each channel, maximum Z-stack projections were made and processed with ImageJ.

209

210 **Chicken type I IFN bioassay.**

211 Bioactive chicken type I interferon (chIFN) was measured using a bioassay based on the CEC-32
212 quail reporter cell line expressing luciferase under the control of the chicken *Mx* promotor (47)
213 (kindly provided by Prof. Peter Staeheli). Briefly, CEC-32 were incubated with serial dilutions of
214 chIFN-containing samples for 6 hours, after which luciferase activity was quantified and IFN
215 concentrations calculated using a chIFN standard. To avoid influence of IBV on the assay, samples
216 were heat inactivated at 56°C for 30 min, which did not influence type I chIFN bioactivity.

217

218 **Gene silencing**

219 siRNAs targeting chicken *Tlr3* and *Mda5* were designed by and purchased from Microsynth,
220 Switzerland (sequences in Table 1). Transfections were performed using siLentFect (Biorad) at a
221 final siRNA concentration of 20 nM. For one well, 160 ng siRNA was combined with 1 μL siLentFect
222 in 100 μL OptiMEM (Gibco) and incubated for 20 min. The siRNA complexes were added to 2×10^5
223 DF-1 cells grown in 500 μL medium per well in a 24 well plate. siRNA complexes were left on the
224 cells for 48 hours before further experiments were performed.

225

226 **Statistics**

227 All statistical analyses were performed in GraphPad Prism 5.0. RT-qPCR fold changes were first log
228 transformed and then used for statistical analysis. For all tests, equality of variance was assessed
229 using Bartlett's test. Significant differences ($P < 0.01$) were determined by a one way or two-way
230 ANOVA (indicated in the figure legend) followed by a Bonferroni post-hoc test.

231

232

233 **Results**

234

235 **IBV delays the onset of an IFN response during infection of primary chicken cells**

236 To investigate the kinetics of viral replication and IFN induction upon infection with the avian
237 *Gammacoronavirus* IBV, we infected primary CEK cells (24) with the IBV M41 strain. To monitor
238 the kinetics of the IFN response in relation to IBV replication, we quantified transcription of *Ifnβ*, a
239 set of genes involved in innate immunity, extracellular IFN protein production, virus titres and IBV
240 RNA in M41-infected CEK cells. In line with previous observations (48), progeny virus was produced
241 after 6 hpi and virus titres reached a maximum around 24 hpi (Fig. 1A). Total intracellular IBV RNA
242 levels reflected the kinetics of infectious IBV virus in the supernatant (Fig. 1A), reaching maximum
243 levels around 24 hpi. *Ifnβ* expression was delayed with respect to the peak of viral replication and
244 remained low until 18 hpi, after which it was strongly upregulated, peaking around 36 hpi (Fig.
245 1B). IFN protein activity levels were quantified using a chicken IFN-specific *Mx-luc* cell-based
246 bioassay showing accumulation of IFN from 36 hpi onwards (Fig. 1B). Concomitant with *Ifnβ*, a
247 subset of genes involved in innate immunity, including *Mx*, *Oas* and *Ii8*, were upregulated whereas
248 others, such as *Tlr7*, *Adar*, *Isg12*, *MHC-I* and *Ifnar2* appeared not, or only marginally affected by
249 IBV infection (Fig. 1C). Pattern recognition receptors *Mda5* and *Tlr3* and the transcription factor
250 *Irf3* were also upregulated (Fig. 1C), which is of interest given the role of these PRRs in virus
251 recognition.

252

253 **The delayed IFN response is independent from the cell type or virus strain**

254 *Ifnβ* transcription during infection with coronaviruses such as MHV and SARS-CoV is generally low
255 (9, 10, 12, 13, 49), and was shown to be dependent on cell type and virus strain (50). The delayed
256 induction of *Ifnβ* transcription observed in IBV M41-infected CEK cells prompted us to investigate
257 whether induction of *Ifnβ* would be dependent on the cell type or IBV strain. Epithelial cells isolated
258 from trachea of 10-week-old SPF chickens and DF-1 chicken fibroblast cells were infected with IBV
259 M41 or IBV Beaudette (Beau-R, (38)). At several time points after infection, *Ifnβ* levels were
260 monitored by RT-qPCR (Fig. 2A and 2B). In both cell types *Ifnβ* transcription followed the same
261 kinetics observed in CEK cells (Fig. 1B), indicating that induction of *Ifnβ* by IBV is independent of
262 cell type. To study whether induction of *Ifnβ* transcription differs between different strains of IBV,
263 we also infected CEK cells with the QX and ItO2 strains of IBV (Fig. 2C). Although we observed
264 some differences in absolute levels of *Ifnβ* upregulation induced by QX, ItO2 and M41, kinetics of

265 *Ifn β* transcription were similar, suggesting that delayed induction of *Ifn β* transcription could be
266 considered a general feature of IBV infection in chicken cells.

267 To assess whether CEK and DF-1 cells do have the intrinsic ability to express *Ifn β* earlier than 18h,
268 we stimulated these cells with extracellular polyI:C (pI:C), transfected pI:C (t[pI:C]) or with the
269 dsRNA virus Infectious Pancreatic Necrosis Virus (IPNV). We found that stimulation of CEK cells
270 with pI:C could induce *Ifn β* transcription as early as one hour after stimulation (Fig. 3A). In DF-1
271 cells, stimulation with IPNV, and t[pI:C], but not pI:C, induced *Ifn β* already at 4h (Fig. 3B). The
272 observation that DF-1 cells do not respond to stimulation with extracellular dsRNA, is in accordance
273 with previous findings and is most likely due to the lack of surface expression of TLR3 (51). In
274 addition, a 12h infection of CEK cells with Sindbis, IPNV or Rift Valley Fever Virus clone 13 (RVFV
275 Cl13) induced a clear transcription of *Ifn β* (Fig. 3C). These results suggest that delayed expression
276 of *Ifn β* is a specific feature of IBV infection and not an intrinsic characteristic of chicken cells.

277

278 **The intracellular pattern recognition receptor MDA5 is the primary sensor of IBV**

279 In general, dsRNA has been shown to be the canonical inducer of *Ifn β* during infection with *Alpha*-
280 and *Betacoronaviruses* (16, 50). To determine which pattern recognition receptor (PRR) would be
281 involved in sensing (ds)RNA of the *Gammacoronavirus* IBV, leading to subsequent *Ifn β*
282 transcription, we first examined the possibility that IBV-(ds)RNA could be sensed extracellularly by,
283 for example, cell-surface receptors. To investigate this, CEK cells were infected with IBV M41 in the
284 presence of RNase A and *Ifn β* expression was analysed. As a positive control, CEK cells were
285 stimulated with pI:C in the presence or absence of RNase A. The IFN response to pI:C was greatly
286 inhibited by addition of RNase A, which had no effect on *Ifn β* levels induced by infection with IBV
287 M41 (Fig. 4A). These data suggest that *Ifn β* upregulation during the late stage (>18 hpi) of IBV
288 infection could be the result of sensing of IBV-(ds)RNA by an intracellular rather than an
289 extracellular pattern recognition receptor. This is consistent with our observation that IBV infection
290 can be detected by DF-1 cells, which show only a marginal upregulation of *Ifn β* transcription in
291 response to extracellular dsRNA (see Fig. 3B). In general, dsRNA can be recognised by membrane-
292 bound TLR3 and cytosolic RLRs such as MDA5 and RIG-I. Genome mining strongly indicates that
293 chickens do not express a *RIG-I* homologue (52), leaving TLR3 and MDA5 as the two PRRs
294 potentially involved in dsRNA sensing. Silencing of *Mda5*, but not *Tlr3*, in DF-1 cells resulted in a
295 70% decrease in *Ifn β* transcription (Fig. 4B). Similar results were obtained with an *Ifn β* -luc DF-1
296 reporter cell line in which silencing of *Mda5*, but not *Tlr3*, resulted in a 70% decrease in luciferase

297 activity by the reporter cells (Fig. 4C). Because no antibody against chicken MDA5 is currently
298 available for protein detection, successful knockdown was evaluated using RT-qPCR demonstrating
299 a silencing efficiency for both *Tlr3* and *Mda5* of approximately 60% (data not shown). Replication of
300 IBV at the investigated time point was not affected by knockdown of neither *Tlr3* nor *Mda5*, as
301 measured by both virus titre and intracellular IBV total RNA (Fig. 4D). These results indicate that
302 MDA5 is the primary PRR responsible for sensing *Gammacoronavirus* IBV-(ds)RNA in chicken cells.

303

304 **Early accumulation of dsRNA in IBV-infected cells does not result in early induction of**
305 ***Ifnβ***

306 Having assessed that chicken cells can indeed promptly respond to stimulation with dsRNA (Fig. 3)
307 and having identified MDA5 as the primary sensor involved in the detection of IBV (Fig. 4), we
308 investigated whether there would be a temporal difference between IBV-induced accumulation of
309 dsRNA and the upregulation of *Ifnβ* transcription in CEK cells. Indeed, dsRNA could clearly be
310 detected, even at low MOI of 0.01, by 12 hpi (Fig. 5A). In contrast, *Ifnβ* levels at this time point
311 remained low (Fig. 5B) even in cell cultures infected at higher MOIs of 1 or 10 and despite the
312 increased abundance of dsRNA. To further investigate the time lag between early accumulation of
313 dsRNA and late *Ifnβ* expression, we performed a time course analysis. Foci of dsRNA could be
314 detected as early as 3 hours post-infection only in IBV-infected cells (Fig. 5C, inset 3hpi) indicating
315 that dsRNA starts accumulating very early in IBV-infected cells but apparently only leads to late
316 (>18 hpi) *Ifnβ* transcription.

317 Primary CEK cells consist of a heterogeneous mix of cell types. Even at high MOI, IBV M41 infects
318 only ~70% of the cells, indicating that not all cells are permissive to IBV M41 infection. In order to
319 assess whether the time lag between accumulation of dsRNA and *Ifnβ* expression could be due to
320 the induction of *Ifnβ* in bystander rather than IBV-infected cells, we used RNA fluorescent *in situ*
321 hybridisation to visualise *Ifnβ* mRNA in IBV-infected CEK cell cultures (Fig. 5D). At 12 hpi and low
322 MOI (0.1), with most cells showing clear foci of dsRNA, none of the IBV-infected cells displayed an
323 accumulation of *Ifnβ* mRNA. At 12 hpi and a higher MOI, a few cells stained positive for *Ifnβ* mRNA
324 and only later, at 24 hpi, did most IBV-infected cells also stain positive for *Ifnβ* mRNA, the kinetics
325 of which closely following that observed in Figure 5A. In all cases, detection of *Ifnβ* mRNA was
326 restricted to cells that contained dsRNA. Altogether our data shows that IBV-infected, but not
327 adjacent uninfected cells, upregulate *Ifnβ* transcription in response to IBV infection. The significant

328 time lag between accumulation of dsRNA and *Ifnβ* transcription further suggests the presence of a
329 mechanism adopted by IBV to circumvent the onset of an IFN response.

330

331 **Accessory proteins 3a and 3b regulate IFN transcription and protein production**

332 To investigate whether the accessory proteins of IBV might play a role in the observed delay in *Ifnβ*
333 transcription, we infected CEK cells with IBV scAUG3ab and scAUG5ab null viruses and the parental
334 Beau-R virus (scAUG viruses possess a scrambled AUG start codon resulting in transcription but not
335 translation of either ORFs 3a and 3b or 5a and 5b (36, 37)). Infection with the scAUG3ab, but not a
336 scAUG5ab null virus resulted by 24 hpi in increased upregulation of *Ifnβ* expression (Fig. 6A).
337 Indicating that either one, or a combination of, accessory proteins 3a and 3b play a role in down
338 regulating *Ifnβ* transcription. The difference in *Ifnβ* transcription between the scAUG3ab and the
339 parental (Beau-R) virus could not be ascribed to differences in kinetics of virus replication, as all
340 viruses displayed similar growth kinetics until 24 hpi (Fig. 6B). To determine whether 3a, 3b or
341 both accessory proteins are involved in the observed down regulation of the IFN response, we
342 quantified *Ifnβ* transcription and IFN protein production in CEK cells infected with scAUG3a,
343 scAUG3b and scAUG3ab mutant viruses, and compared the values observed in cells infected with
344 Beau-R (Fig. 6C and 6D). Infection with all mutant viruses led to an increased transcription of *Ifnβ*
345 when compared to the Beau-R (Fig. 6C), indicating that the presence of either one of the two
346 accessory proteins is sufficient to limit *Ifnβ* transcription. The kinetics of *Ifnβ* transcription in
347 response to AUG3a/b differs between Fig. 6A and Fig. 6C. In Fig 6C there is a significant difference
348 in *Ifnβ* transcription between AUG3a/b and Beau-R, which is absent in Fig 6A. This difference can
349 probably be attributed to variation in the kinetics of *Ifnβ* transcription between primary CEK cells
350 isolated from embryos originating from different flocks. Nonetheless, this difference does not affect
351 the conclusion that knockout of 3a and 3b leads to an increase in transcription of *Ifnβ*.
352 No significant differences in IFN protein production were observed between cells infected with the
353 Beau-R and the scAUG3ab double null virus, except at 36 hpi. However, infection with scAUG3b
354 virus led to an increase in IFN protein levels, whereas infection with the scAUG3a virus led to a
355 decrease in IFN when compared to both Beau-R and scAUG3ab double null virus (Fig. 6D). Taken
356 together, these results indicate that accessory proteins 3a and 3b both play a role in the inhibition
357 of *Ifnβ* transcription but have distinct and opposing effects on protein production. Accessory protein
358 3b seems to be involved in limiting IFN protein activity whereas 3a is involved in promoting it.

359

360 **Signalling of non-self dsRNA remains intact in IBV-infected cells**

361 Since IBV showed the intrinsic ability to delay *Ifn β* transcription in several cell types (Fig. 1 and
362 Fig. 2) even in the presence of high levels of intracellular dsRNA (Fig. 5), we investigated the
363 ability of IBV to interfere with sensing of non-self dsRNA by TLR3 or MDA5. We infected CEK cells
364 with IBV M41 and subsequently used extracellular poly I:C to trigger TLR3 signalling (Fig. 7A).
365 Stimulation with pI:C alone led to a significant increase in *Ifn β* transcription whereas stimulation
366 with pI:C following an infection with IBV led to an enhanced increase in *Ifn β* transcription in an
367 MOI-dependent manner. These results indicated that IBV infection does not interfere with TLR3-
368 mediated *Ifn β* transcription, on the contrary IBV infection appears to result in a synergistic
369 activation of the TLR3 pathway triggered by pI:C. Next, we investigated whether IBV infection
370 could interfere with MDA5-mediated transcription of *Ifn β* . Although transfection of pI:C into the
371 intracellular compartment is a commonly used ligand of MDA5, this method induced very little
372 transcription of *Ifn β* in primary CEK cells, because of low transfection efficiency (data not shown).
373 As an alternative route to stimulate MDA5 in primary chicken cells, we investigated the use of
374 either RVFV CI13 or IPNV, that induce *Ifn β* transcription in CEK cells (Fig 3C). RVFV CI13 is a (-)
375 ssRNA virus with a truncated IFN antagonist (53), for which RIG-I, but not by MDA5 or TLR3, was
376 previously shown to be the most likely PRR in mammalian cells (54, 55). Since chickens, as
377 opposed to most mammals, do not have a *RIG-I* homologue, the most likely PRR for RVFV in CEK
378 cells would be MDA5. IPNV is a birnavirus with a dsRNA genome that naturally infects salmonids
379 but has been shown to enter but not replicate in cells of warm-blooded animals (56). To date, the
380 PRR responsible for sensing IPNV dsRNA has not been described. Knockdown experiments in DF-1
381 *Ifn β* -luc reporter cells, using siRNAs against chicken MDA5 or TLR3, revealed that MDA5, but not
382 TLR3, is the prime PRR for IPNV (Fig. 7B). These findings were confirmed using MEFs (mouse
383 embryo fibroblasts) from knockout mice deficient in expression of either MDA5, RIG-I or the
384 downstream adaptor protein MAVS. Here, knockout of either MDA5 or MAVS abrogated sensing of
385 IPNV as shown by a strong reduction of *Ifn β* transcription, whereas knockout of RIG-I did not (Fig.
386 7C). Both IPNV and RVFV CI13 were subsequently used to investigate whether IBV infection could
387 interfere with MDA5-mediated transcription of *Ifn β* in CEK cells.

388 Using quantification of *Ifn β* transcription by RT-qPCR as read out, we could show that IBV infection
389 does not interfere with MDA5-mediated signalling of IPNV (Fig. 7D) or RVFV CI13 (Fig. 7E), in fact
390 it had a synergistic effect on *Ifn β* transcription as previously observed for TLR3-mediated signalling
391 (Fig. 7A). Similar results were obtained when stimulating IBV-infected DF-1 cells with IPNV or

392 t[pI:C] (Fig. 7F), indicating that the observed synergistic effect is not specific to CEK cells. Taken
393 together, IBV infection very efficiently prevents sensing of IBV (ds)RNA, but our results indicate
394 that it does not interfere with sensing and downstream signalling of other non-self (ds)RNA ligands.

395

396 **DISCUSSION**

397 In this study we performed a comprehensive analysis of the kinetics of IBV infection in avian cells
398 and studied the mechanisms by which IBV interferes with the onset of the type I IFN response. We
399 show that infection with the *Gammacoronavirus* IBV leads to a considerable activation of the type I
400 IFN response, albeit delayed with respect to the peak of viral replication and accumulation of viral
401 dsRNA. Using an siRNA knockdown approach we show that MDA5 is the main receptor involved in
402 the induction of *Ifn β* expression during IBV infection. We present evidence that IBV accessory
403 proteins 3a and 3b play a role in the modulation of the delayed IFN response, by regulating
404 interferon production both at the transcriptional as well as translational level. In addition, we show
405 that although IBV alone effectively prevents *Ifn β* induction in IBV-infected cells, it does not block
406 *Ifn β* induction upon stimulation of IBV-infected cells with other RIG-I, MDA5 or TLR3 ligands. To
407 our knowledge, this study provides the most comprehensive analysis of the interplay between a
408 *Gammacoronavirus* and the avian type I IFN response.

409

410 Much of our current knowledge about the interaction of coronaviruses with the innate immune
411 response (reviewed in (57)) comes from studies in mice and mouse cells using mouse hepatitis
412 virus (MHV). MHV activated IFN production only in specific cell types and an efficient IFN response
413 was only mounted by plasmacytoid dendritic cells (58), bone marrow derived macrophages (10,
414 59) and oligodendrocytes (10). In a recent study on SARS-CoV and MERS-CoV in an epithelial lung
415 cell line, ISGs started to be upregulated at 12 hpi (60), when virus titres were already reaching
416 their maximum. The kinetics of IFN response observed in our study are in line with aforementioned
417 studies, however it must be noted that in most cell types, infection with *Alpha* or *Betacoronaviruses*
418 induced very little, if any, *Ifn β* transcription (8-13, 49). This suggests that all coronaviruses are
419 able to modulate the activation of the type I IFN response.

420

421 We found that IBV infection is detected by various chicken cell types, but until now it was unknown
422 which PRR was involved. MHV has been shown to be detected by MDA5 and not RIG-I or TLR3 in
423 brain macrophages (50), by both MDA5 and RIG-I in an oligodendrocyte derived cell line (10) and

424 by TLR7 in plasmacytoid dendritic cells (58). Analysis of the chicken genome suggests that chicken
425 lack a *RIG-I* homologue (52), and basal expression of *Tlr7* was found to be very low in CEK cells
426 (data not shown). We therefore silenced the remaining candidate RNA sensors MDA5 and TLR3,
427 and were able to show that MDA5, but not TLR3, is involved in the sensing of IBV. Silencing of
428 *Mda5* did not lead to an increase in replication of IBV, suggesting that IBV might have developed
429 strategies to counteract the activated IFN response.

430

431 We recently reported membrane rearrangements in chicken cells infected with IBV (48), similar to
432 those found in cells infected with *Betacoronaviruses*. In theory, the formation of intracellular
433 membrane rearrangements might partly explain the discrepancy observed in the kinetics of dsRNA
434 accumulation and *Ifn β* upregulation. Indeed, for SARS-CoV it has been shown that virus-induced
435 double membrane vesicles (DMVs) contain dsRNA (14), suggesting that coronaviruses might
436 exploit membrane structures to shield dsRNA from recognition by host PRRs (61). However, the
437 kinetics of *Ifn β* transcription were not investigated in these studies. The presence of coronavirus-
438 induced DMVs has been demonstrated as early as 2 hpi in SARS-CoV-infected cells (14). Although
439 we did not demonstrate the presence of DMVs in IBV-infected chicken cells at time points earlier
440 than 7 hpi (48), it is likely that DMVs could also be present at earlier time points. As such, the
441 timing of DMV formation in coronavirus-infected cells could suggest that membrane
442 rearrangements play a role in the delayed activation of the IFN response by shielding dsRNA from
443 cellular PRRs.

444

445 In addition to membrane rearrangements, coronavirus-encoded proteins, including numerous
446 accessory genes, have been shown to interfere with the type I IFN response pathway (reviewed in
447 (17, 18). To investigate the possible role of IBV accessory proteins in the regulation of the IFN
448 response we made use of our previously constructed mutant IBV Beau-R viruses that do not
449 express either one or more of the four accessory proteins 3a, 3b, 5a and 5b. Previously we have
450 demonstrated the accessory genes of IBV are not essential for replication (36, 37). In the present
451 study we show that infection of CEK cells with 3a or 3b null viruses as well as a 3a/3b double null
452 virus led to increased *Ifn β* transcription compared to Beau-R. Because the kinetics of *Ifn β*
453 transcription of 3a, 3b and 3a/3b null viruses are comparable to the parental virus, we conclude
454 that, 3a and 3b are probably not responsible for the delay in *Ifn β* transcription, suggesting that IBV
455 utilises additional strategies to delay transcription of *Ifn β* . Apart from their effect on *Ifn β*

456 transcription, 3a and 3b seem to have opposing effects on IFN protein production by IBV infected
457 cells. Infection with the 3b null virus resulted in increased IFN production whereas infection with
458 the 3a null virus resulted in reduced IFN levels compared to the Beau-R virus. Together with the
459 observation that IFN production induced by the 3a/3b double null virus is comparable to that
460 induced by Beau-R virus, our data suggests that accessory proteins 3a and 3b antagonise each
461 other to tightly regulate IFN production (Fig. 6B).

462

463 Using the eukaryotic linear motif server (62), we identified a Protein phosphatase 1 (PP1)-binding
464 ¹⁷KISF²⁰ domain in the IBV 3b protein sequence. The canonical PP1-binding motif is
465 [R/K][V/I/L]X[F/W], in which x can be any amino acid except proline (63). Interestingly,
466 *Alphacoronavirus* TGEV accessory protein 7 (TGEV-7) has been shown to bind PP1 via a binding
467 motif similar to that found in IBV 3b (64). Similar to IBV scAUG3b, infection with TGEV-Δ7 led to
468 increased mRNA and protein levels of IFNβ (65). The fact that both TGEV-7 and IBV 3b contain a
469 PP1 binding domain indicates that interaction with PP1 could be a common strategy of
470 coronaviruses to inhibit the host innate immune response. The mechanism by which interaction of
471 coronavirus accessory proteins with PP1 counteracts the innate immune response still needs to be
472 determined. One clue might come from the PP1-binding domain of Measles virus V, which was
473 recently shown to be essential for inhibition of MDA5 signalling (66, 67). Measles V protein binds
474 PP1 and inhibits dephosphorylation of MDA5, which is required for activation and subsequent
475 signalling by MDA5. Motif analysis for IBV 3a protein did not reveal the presence of relevant
476 motives that might explain the observed activity of 3a on IFN regulation. We conclude that both
477 accessory proteins 3a and 3b limit *Ifnβ* transcription but have distinct and opposing effects on
478 protein production. Whilst 3a seems to promote IFN production, 3b seems to be involved in limiting
479 IFN protein production, possibly through a similar mechanism as described for protein 7 of TGEV.
480 The fact that IBV 3a and 3b have opposing roles in regulating IFN production indicates that CoV's
481 tightly regulate IFN production to balance their own survival with that of the host. This hypothesis
482 is supported by the observation that field isolates lacking 3a and 3b display reduced virulence *in*
483 *vitro* as well as *in vivo* (68). Elucidation of the exact mechanisms of action of 3a and 3b will be the
484 subject of further investigation.

485

486

487 To investigate whether IBV interferes with a general sensing of (ds)RNA ligands or downstream
488 signalling that leads to *Ifn β* transcription, we stimulated IBV-infected cells with TLR3, RIG-I, and
489 MDA5 ligands. Surprisingly, we found that infection with IBV did not reduce *Ifn β* transcription but
490 rather increased *Ifn β* levels upon stimulation with these PRR ligands. Similar to IBV, MHV has been
491 shown unable to inhibit expression of *Ifn β* induced by either t[pI:C] or Sendai virus (69, 70), but in
492 these studies no synergistic effect was observed. Currently, we can only speculate about the cause
493 of this synergistic effect. It appears that IBV infection 'arms' the *Ifn β* induction pathway, without
494 actually triggering it, possibly by enhancing the activity of one or more components of the pathway
495 leading to *Ifn β* upregulation. One possibility is that IBV-proteins interact with host-proteins that
496 regulate this pathway through ubiquitination and phosphorylation (reviewed in (71)). The fact that
497 stimulation with either TLR3 or MDA5 ligands resulted in exacerbated transcription of *Ifn β* indicates
498 that IBV influences a component which is downstream of both MDA5 and TLR3.

499

500 Taken together, our study provides the first comprehensive analysis of host-virus interactions of a
501 *Gammacoronavirus* with the avian innate immune response. We show that the *Gammacoronavirus*
502 IBV, induces activation of the type I IFN response in primary chicken renal cells, tracheal epithelial
503 cells and in a chicken cell line. We show that activation of the IFN response is dependent on MDA5
504 but is delayed with respect to the peak of virus replication. We demonstrate that *Ifn β* transcription
505 is restricted to IBV-infected, dsRNA-containing cells and provide evidence that accessory proteins
506 3a and 3b of IBV are involved in regulating transcription as well as protein production of type I IFN.

507

508 **Acknowledgements:** The authors would like to thank Peter Staeheli of the University of Freiburg
509 for providing the chicken interferon reporter cell line and chIFN standard. Marleen Scheer and Lieke
510 Golbach from the Cell Biology and Immunology Group of Wageningen University for technical
511 assistance in the RNA silencing experiment and assistance in microscopy and image processing,
512 respectively. Gorben Pijlman from the Virology Group of Wageningen University and Marjolein
513 Kikkert of the Molecular Virology Laboratory of Leiden University Medical Center are gratefully
514 acknowledged for their critical discussions on the manuscript. This work was financially supported
515 by MSD Animal Health, Bioprocess Technology & Support, Boxmeer, The Netherlands. Helena Maier
516 and Paul Britton were supported by The Pirbright Institute and the Biotechnology and Biological
517 Sciences Research Council (BBSRC).

518

- 520 1. **Cavanagh D.** 2007. Coronavirus avian infectious bronchitis virus. *Vet Res* **38**:281-297.
- 521 2. **Thiel V.** 2007. Coronaviruses: Molecular and Cellular Biology. Horizon Scientific Press.
- 522 3. **Cavanagh D.** 2005. Coronaviruses in poultry and other birds. *Avian Pathol* **34**:439-448.
- 523 4. **Cook JK, Jackwood M, Jones RC.** 2012. The long view: 40 years of infectious bronchitis research. *Avian Pathol* **41**:239-250.
- 524 5. **Jones RC.** 2010. Viral respiratory diseases (ILT, aMPV infections, IB): are they ever under control? *British Poultry Science* **51**:1-11.
- 525 6. **Saif YM, Barnes HJ.** 2008. Diseases of poultry, 12th ed. Blackwell Pub. Professional, Ames, Iowa.
- 526 7. **Barbalat R, Ewald SE, Mouchess ML, Barton GM.** 2011. Nucleic acid recognition by the innate immune system. *Annual review of immunology* **29**:185-214.
- 527 8. **Rose KM, Elliott R, Martinez-Sobrido L, Garcia-Sastre A, Weiss SR.** 2010. Murine coronavirus delays expression of a subset of interferon-stimulated genes. *J Virol* **84**:5656-5669.
- 528 9. **Devaraj SG, Wang N, Chen Z, Tseng M, Barretto N, Lin R, Peters CJ, Tseng CT, Baker SC, Li K.** 2007. Regulation of IRF-3-dependent innate immunity by the papain-like protease domain of the severe acute respiratory syndrome coronavirus. *J Biol Chem* **282**:32208-32221.
- 529 10. **Li J, Liu Y, Zhang X.** 2010. Murine Coronavirus Induces Type I Interferon in Oligodendrocytes through Recognition by RIG-I and MDA5. *J. Virol.* **84**:6472-6482.
- 530 11. **Kindler E, Jonsdottir HR, Muth D, Hamming OJ, Hartmann R, Rodriguez R, Geffers R, Fouchier RA, Drosten C, Muller MA, Dijkman R, Thiel V.** 2013. Efficient Replication of the Novel Human Betacoronavirus EMC on Primary Human Epithelium Highlights Its Zoonotic Potential. *mBio* **4**.
- 531 12. **Zhao L, Rose KM, Elliott R, Van Rooijen N, Weiss SR.** 2011. Cell-type-specific type I interferon antagonism influences organ tropism of murine coronavirus. *J Virol* **85**:10058-10068.
- 532 13. **Roth-Cross JK, Martinez-Sobrido L, Scott EP, Garcia-Sastre A, Weiss SR.** 2007. Inhibition of the alpha/beta interferon response by mouse hepatitis virus at multiple levels. *J Virol* **81**:7189-7199.
- 533 14. **Knoops K, Kikkert M, Worm SH, Zevenhoven-Dobbe JC, van der Meer Y, Koster AJ, Mommaas AM, Snijder EJ.** 2008. SARS-coronavirus replication is supported by a reticulovesicular network of modified endoplasmic reticulum. *PLoS biology* **6**:e226.
- 534 15. **Gosert R, Kanjanahaluethai A, Egger D, Bienz K, Baker SC.** 2002. RNA replication of mouse hepatitis virus takes place at double-membrane vesicles. *J Virol* **76**:3697-3708.
- 535 16. **Zust R, Cervantes-Barragan L, Habjan M, Maier R, Neuman BW, Ziebuhr J, Szretter KJ, Baker SC, Barchet W, Diamond MS, Siddell SG, Ludewig B, Thiel V.** 2011. Ribose 2'-O-methylation provides a molecular signature for the distinction of self and non-self mRNA dependent on the RNA sensor Mda5. *Nature immunology* **12**:137-143.
- 536 17. **Zhong Y, Tan YW, Liu DX.** 2012. Recent progress in studies of arterivirus- and coronavirus-host interactions. *Viruses* **4**:980-1010.
- 537 18. **Liu DX, Fung TS, Chong KK-L, Shukla A, Hilgenfeld R.** 2014. Accessory proteins of SARS-CoV and other coronaviruses. *Antiviral Research* **109**:97-109.
- 538 19. **Holmes HC, Darbyshire JH.** 1978. Induction of chicken interferon by avian infectious bronchitis virus. *Res Vet Sci* **25**:178-181.
- 539 20. **Lomniczi B.** 1974. Interferon induction by different strains of infectious bronchitis virus. *Acta veterinaria Academiae Scientiarum Hungaricae* **24**:199-204.
- 540 21. **Otsuki K, Nakamura T, Kawaoka Y, Tsubokura M.** 1988. Interferon induction by several strains of avian infectious bronchitis virus, a coronavirus, in chickens. *Acta Virol* **32**:55-59.
- 541 22. **Otsuki K, Nakamura T, Kubota N, Kawaoka Y, Tsubokura M.** 1987. Comparison of two strains of avian infectious bronchitis virus for their interferon induction, viral growth and development of virus-neutralizing antibody in experimentally-infected chickens. *Veterinary microbiology* **15**:31-40.
- 542 23. **Dar A, Munir S, Vishwanathan S, Manuja A, Griebel P, Tikoo S, Townsend H, Potter A, Kapur V, Babiuk LA.** 2005. Transcriptional analysis of avian embryonic tissues following infection with avian infectious bronchitis virus. *Virus Res* **110**:41-55.
- 543 24. **Wang X, Rosa AJ, Oliverira HN, Rosa GJ, Guo X, Travnicek M, Girshick T.** 2006. Transcriptome of local innate and adaptive immunity during early phase of infectious bronchitis viral infection. *Viral Immunol* **19**:768-774.
- 544 25. **Cong F, Liu X, Han Z, Shao Y, Kong X, Liu S.** 2013. Transcriptome analysis of chicken kidney tissues following coronavirus avian infectious bronchitis virus infection. *BMC Genomics* **14**:743.
- 545 26. **Li FQ, Tam JP, Liu DX.** 2007. Cell cycle arrest and apoptosis induced by the coronavirus infectious bronchitis virus in the absence of p53. *Virology* **365**:435-445.
- 546 27. **Liu C, Xu HY, Liu DX.** 2001. Induction of caspase-dependent apoptosis in cultured cells by the avian coronavirus infectious bronchitis virus. *J Virol* **75**:6402-6409.
- 547 28. **Xiao H, Xu LH, Yamada Y, Liu DX.** 2008. Coronavirus spike protein inhibits host cell translation by interaction with eIF3f. *PLoS One* **3**:e1494.
- 548 29. **Wang X, Liao Y, Yap PL, Png KJ, Tam JP, Liu DX.** 2009. Inhibition of protein kinase R activation and upregulation of GADD34 expression play a synergistic role in facilitating coronavirus replication by maintaining de novo protein synthesis in virus-infected cells. *J Virol* **83**:12462-12472.
- 549 30. **Emeny JM, Morgan MJ.** 1979. Regulation of the Interferon System - Evidence That Vero Cells Have a Genetic Defect in Interferon-Production. *Journal of General Virology* **43**:247-252.
- 550 31. **Mosca JD, Pitha PM.** 1986. Transcriptional and posttranscriptional regulation of exogenous human beta interferon gene in simian cells defective in interferon synthesis. *Mol Cell Biol* **6**:2279-2283.

- 587 32. **Hodgson T, Casais R, Dove B, Britton P, Cavanagh D.** 2004. Recombinant infectious bronchitis
588 coronavirus Beaudette with the spike protein gene of the pathogenic M41 strain remains attenuated
589 but induces protective immunity. *J Virol* **78**:13804-13811.
- 590 33. **Kato H, Takeuchi O, Mikamo-Satoh E, Hirai R, Kawai T, Matsushita K, Hiiragi A, Dermody TS,**
591 **Fujita T, Akira S.** 2008. Length-dependent recognition of double-stranded ribonucleic acids by
592 retinoic acid-inducible gene-I and melanoma differentiation-associated gene 5. *J Exp Med* **205**:1601-
593 1610.
- 594 34. **Bhoj VG, Sun Q, Bhoj EJ, Somers C, Chen X, Torres JP, Mejias A, Gomez AM, Jafri H, Ramilo**
595 **O, Chen ZJ.** 2008. MAVS and MyD88 are essential for innate immunity but not cytotoxic T lymphocyte
596 response against respiratory syncytial virus. *Proc Natl Acad Sci U S A* **105**:14046-14051.
- 597 35. **Fitzgerald KA, McWhirter SM, Faia KL, Rowe DC, Latz E, Golenbock DT, Coyle AJ, Liao SM,**
598 **Maniatis T.** 2003. IKKepsilon and TBK1 are essential components of the IRF3 signaling pathway.
599 *Nature immunology* **4**:491-496.
- 600 36. **Hodgson T, Britton P, Cavanagh D.** 2006. Neither the RNA nor the proteins of open reading frames
601 3a and 3b of the coronavirus infectious bronchitis virus are essential for replication. *Journal of virology*
602 **80**:296-305.
- 603 37. **Casais R, Davies M, Cavanagh D, Britton P.** 2005. Gene 5 of the avian coronavirus infectious
604 bronchitis virus is not essential for replication. *Journal of virology* **79**:8065-8078.
- 605 38. **Casais R, Thiel V, Siddell SG, Cavanagh D, Britton P.** 2001. Reverse genetics system for the avian
606 coronavirus infectious bronchitis virus. *J Virol* **75**:12359-12369.
- 607 39. **Liniger M, Summerfield A, Zimmer G, McCullough KC, Ruggli N.** 2012. Chicken cells sense
608 influenza A virus infection through MDA5 and CARDIF signaling involving LGP2. *J Virol* **86**:705-717.
- 609 40. **Villanueva AI, Kulkarni RR, Sharif S.** 2011. Synthetic double-stranded RNA oligonucleotides are
610 immunostimulatory for chicken spleen cells. *Dev Comp Immunol* **35**:28-34.
- 611 41. **Li YP, Handberg KJ, Juul-Madsen HR, Zhang MF, Jorgensen PH.** 2007. Transcriptional profiles of
612 chicken embryo cell cultures following infection with infectious bursal disease virus. *Archives of*
613 *virology* **152**:463-478.
- 614 42. **Daviet S, Van Borm S, Habyarimana A, Ahanda M-LE, Morin V, Oudin A, Van Den Berg T,**
615 **Zoorob R.** 2009. Induction of Mx and PKR Failed to Protect Chickens from H5N1 Infection. *Viral*
616 *Immunology* **22**:467-472.
- 617 43. **Forlenza M, Kaiser T, Savelkoul HF, Wiegertjes GF.** 2012. The use of real-time quantitative PCR
618 for the analysis of cytokine mRNA levels. *Methods Mol Biol* **820**:7-23.
- 619 44. **Raj A, van den Bogaard P, Rifkin SA, van Oudenaarden A, Tyagi S.** 2008. Imaging individual
620 mRNA molecules using multiple singly labeled probes. *Nature Methods* **5**:877-879.
- 621 45. **Raj A, Tyagi S, Nils GW.** 2010. Chapter 17 - Detection of Individual Endogenous RNA Transcripts In
622 Situ Using Multiple Singly Labeled Probes, p. 365-386, *Methods in Enzymology*, vol. Volume 472.
623 Academic Press.
- 624 46. **Femino AM, Fay FS, Fogarty K, Singer RH.** 1998. Visualization of Single RNA Transcripts in Situ.
625 *Science* **280**:585-590.
- 626 47. **Schwarz H, Harlin O, Ohnemus A, Kaspers B, Staeheli P.** 2004. Synthesis of IFN-beta by virus-
627 infected chicken embryo cells demonstrated with specific antisera and a new bioassay. *Journal of*
628 *interferon & cytokine research : the official journal of the International Society for Interferon and*
629 *Cytokine Research* **24**:179-184.
- 630 48. **Maier HJ, Hawes PC, Cottam EM, Mantell J, Verkade P, Monaghan P, Wileman T, Britton P.**
631 2013. Infectious Bronchitis Virus Generates Spherules from Zippered Endoplasmic Reticulum
632 Membranes. *mBio* **4**.
- 633 49. **Yoshikawa T, Hill TE, Yoshikawa N, Popov VL, Galindo CL, Garner HR, Peters CJ, Tseng CT.**
634 2010. Dynamic innate immune responses of human bronchial epithelial cells to severe acute
635 respiratory syndrome-associated coronavirus infection. *PLoS One* **5**:e8729.
- 636 50. **Roth-Cross JK, Bender SJ, Weiss SR.** 2008. Murine coronavirus mouse hepatitis virus is recognized
637 by MDA5 and induces type I interferon in brain macrophages/microglia. *J Virol* **82**:9829-9838.
- 638 51. **Karpala AJ, Lowenthal JW, Bean AG.** 2008. Activation of the TLR3 pathway regulates IFNbeta
639 production in chickens. *Developmental and comparative immunology* **32**:435-444.
- 640 52. **Barber MRW, Aldridge JR, Webster RG, Magor KE.** 2010. Association of RIG-I with innate
641 immunity of ducks to influenza. *Proceedings of the National Academy of Sciences* **107**:5913-5918.
- 642 53. **Cameron MJ, Kelvin AA, Leon AJ, Cameron CM, Ran L, Xu L, Chu YK, Danesh A, Fang Y, Li Q,**
643 **Anderson A, Couch RC, Paquette SG, Fomukong NG, Kistner O, Lauchart M, Rowe T, Harrod**
644 **KS, Jonsson CB, Kelvin DJ.** 2012. Lack of innate interferon responses during SARS coronavirus
645 infection in a vaccination and reinfection ferret model. *PLoS One* **7**:e45842.
- 646 54. **Habjan M, Andersson I, Klingström J, Schümamm M, Martin A, Zimmermann P, Wagner V,**
647 **Pichlmair A, Schneider U, Mühlberger E, Mirazimi A, Weber F.** 2008. Processing of Genome 5'
648 Termini as a Strategy of Negative-Strand RNA Viruses to Avoid RIG-I-Dependent Interferon Induction.
649 *PLoS One* **3**:e2032.
- 650 55. **Ermiler ME, Yerukhim E, Schriewer J, Schattgen S, Traylor Z, Wespiser AR, Caffrey DR, Chen**
651 **ZJ, King CH, Gale M, Colonna M, Fitzgerald KA, Buller RML, Hise AG.** 2013. RNA Helicase
652 Signaling Is Critical for Type I Interferon Production and Protection against Rift Valley Fever Virus
653 during Mucosal Challenge. *Journal of Virology* **87**:4846-4860.
- 654 56. **Orpetveit I, Kuntziger T, Sindre H, Rimstad E, Dannevig BH.** 2012. Infectious pancreatic necrosis
655 virus (IPNV) from salmonid fish enters, but does not replicate in, mammalian cells. *Virology journal*
656 **9**:228.
- 657 57. **Kindler E, Thiel V.** 2014. To sense or not to sense viral RNA: essentials of coronavirus innate immune
658 evasion. *Current Opinion in Microbiology* **20**:69-75.

- 659 58. **Cervantes-Barragan L, Züst R, Weber F, Spiegel M, Lang KS, Akira S, Thiel V, Ludewig B.**
660 2007. Control of coronavirus infection through plasmacytoid dendritic-cell-derived type I interferon.
661 *Blood* **109**:1131-1137.
- 662 59. **Zhou H, Zhao J, Perlman S.** 2010. Autocrine interferon priming in macrophages but not dendritic
663 cells results in enhanced cytokine and chemokine production after coronavirus infection. *mBio* **1**.
- 664 60. **Menachery VD, Eisfeld AJ, Schafer A, Josset L, Sims AC, Proll S, Fan S, Li C, Neumann G,**
665 **Tilton SC, Chang J, Gralinski LE, Long C, Green R, Williams CM, Weiss J, Matzke MM, Webb-**
666 **Robertson BJ, Schepmoes AA, Shukla AK, Metz TO, Smith RD, Waters KM, Katze MG,**
667 **Kawaoka Y, Baric RS.** 2014. Pathogenic influenza viruses and coronaviruses utilize similar and
668 contrasting approaches to control interferon-stimulated gene responses. *mBio* **5**:e01174-01114.
- 669 61. **Hagemeijer MC, Vonk AM, Monastyrska I, Rottier PJ, de Haan CA.** 2012. Visualizing coronavirus
670 RNA synthesis in time by using click chemistry. *J Virol* **86**:5808-5816.
- 671 62. **Dinkel H, Van Roey K, Michael S, Davey NE, Weatheritt RJ, Born D, Speck T, Kruger D,**
672 **Grebnev G, Kuban M, Strumillo M, Uyar B, Budd A, Altenberg B, Seiler M, Chemes LB, Glavina**
673 **J, Sanchez IE, Diella F, Gibson TJ.** 2014. The eukaryotic linear motif resource ELM: 10 years and
674 counting. *Nucleic Acids Res* **42**:D259-266.
- 675 63. **Wakula P, Beullens M, Ceulemans H, Stalmans W, Bollen M.** 2003. Degeneracy and function of
676 the ubiquitous RVXF motif that mediates binding to protein phosphatase-1. *J Biol Chem* **278**:18817-
677 18823.
- 678 64. **Cruz J, Sola I, Becares M, Alberca B, Plana J, Enjuanes L, Zuniga S.** 2011. Coronavirus gene 7
679 counteracts host defenses and modulates virus virulence. *PLoS Pathog* **7**:e1002090.
- 680 65. **Cruz JL, Becares M, Sola I, Oliveros JC, Enjuanes L, Zuniga S.** 2013. Alphacoronavirus protein 7
681 modulates host innate immune response. *J Virol* **87**:9754-9767.
- 682 66. **Mesman Annelies W, Zijlstra-Willems Esther M, Kaptein Tanja M, de Swart Rik L, Davis**
683 **Meredith E, Ludlow M, Duprex WP, Gack Michaela U, Gringhuis Sonja I, Geijtenbeek**
684 **Teunis BH.** 2014. Measles Virus Suppresses RIG-I-like Receptor Activation in Dendritic Cells via DC-
685 SIGN-Mediated Inhibition of PP1 Phosphatases. *Cell host & microbe* **16**:31-42.
- 686 67. **Davis Meredith E, Wang May K, Rennick Linda J, Full F, Gableske S, Mesman Annelies W,**
687 **Gringhuis Sonja I, Geijtenbeek Teunis BH, Duprex WP, Gack Michaela U.** 2014. Antagonism of
688 the Phosphatase PP1 by the Measles Virus V Protein Is Required for Innate Immune Escape of MDA5.
689 *Cell host & microbe* **16**:19-30.
- 690 68. **Mardani K, Noormohammadi AH, Hooper P, Ignjatovic J, Browning GF.** 2008. Infectious
691 bronchitis viruses with a novel genomic organization. *J Virol* **82**:2013-2024.
- 692 69. **Zhou H, Perlman S.** 2007. Mouse hepatitis virus does not induce Beta interferon synthesis and does
693 not inhibit its induction by double-stranded RNA. *Journal of virology* **81**:568-574.
- 694 70. **Versteeg GA, Bredenbeek PJ, van den Worm SH, Spaan WJ.** 2007. Group 2 coronaviruses
695 prevent immediate early interferon induction by protection of viral RNA from host cell recognition.
696 *Virology* **361**:18-26.
- 697 71. **Gack MU.** 2014. Mechanisms of RIG-I-Like Receptor Activation and Manipulation by Viral Pathogens.
698 *Journal of Virology* **88**:5213-5216.
- 699

700 **FIGURE LEGENDS**

701

702 **FIG 1. IBV infection delays *Ifnβ* upregulation.**

703 Chicken embryo kidney (CEK) cells were infected with IBV M41 at an MOI of 0.1. (A) Replication of
 704 IBV was quantified by titration in cell culture supernatants of infected cells; in a parallel
 705 experiment, intracellular IBV RNA was quantified using RT-qPCR. (B) *Ifnβ* mRNA levels were
 706 determined using RT-qPCR and IFN protein levels using a chicken IFN-specific *mx-luc* cell-based
 707 bioassay, respectively. (C) Expression of genes involved in the antiviral response. All gene
 708 expressions were calculated as fold changes relative to uninfected control cells and normalised
 709 against an external reference gene (luciferase). For IBV total RNA, fold changes were calculated
 710 relative to C_t 30. Depicted are the results of a representative experiment out of three independent
 711 experiments.

712

713 **FIG 2. Delayed induction of *Ifnβ* transcription is independent of cell type or IBV strain.**

714 (A) Epithelial cells from adult chicken trachea were infected with IBV M41 at MOI 0.1. (B)
 715 Fibroblast DF-1 cells were infected with IBV Beau-R at MOI 0.1. (C) CEK cells were infected with
 716 IBV strains M41, QX and It02, at an MOI 0.1. Intracellular IBV total RNA (open diamonds) and *Ifnβ*
 717 mRNA (bars) are depicted as fold changes as assessed by RT-qPCR. Gene expression of *Ifnβ* was
 718 calculated as fold changes relative to uninfected control cells and normalised against an external
 719 reference gene (luciferase).. For IBV total RNA, fold changes were calculated relative to C_t 30. Error
 720 bars indicate standard deviation.

721

722 **FIG 3. Chicken cells have the intrinsic ability to respond rapidly to dsRNA.**

723 (A) CEK cells were seeded in 24 well plates and 48 hours later stimulated with extracellular poly
 724 I:C for the indicated times. (B) DF-1 cells were infected with IPNV, a non-replicating dsRNA virus,
 725 or stimulated with extracellular pI:C or transfected pI:C (t[pI:C]). Four hours later, *Ifnβ* fold
 726 changes were determined by RT-qPCR. Bars represent the mean (plus standard deviation) of
 727 triplicate wells from a representative experiment. Asterisks indicate significant differences (P<0.01)
 728 with respect to the non-stimulated control as assessed by one-way ANOVA followed by a Bonferroni
 729 post-hoc test. (C) CEK cells were infected with IBV M41 (MOI 1), IBV Beau-R, (MOI 1), Sindbis-GFP
 730 (MOI 1), IPNV (MOI 50) and RVFV CI13 (MOI 5). Depicted are *Ifnβ* fold changes at 12 hpi relative
 731 to uninfected control cells as assessed by RT-qPCR.

732

733 FIG 4. MDA5, and not TLR3, is the prime sensor of IBV.

734 (A) CEK cells were infected with IBV M41 for 24 hours, in the presence or absence of RNase A. *Ifnβ*
735 expression was analysed by RT-qPCR. Stimulation with pI:C in the presence or absence of RNase A
736 was included as a positive control. (B,D) DF-1 cells and (C) DF-1 *Ifnβ*-luc reporter cells were
737 transfected with siRNAs against *Tlr3*, *Mda5* or a control siRNA and 48 hours later infected with IBV
738 M41 (MOI 0.1). (B) *Ifnβ* mRNA, (C) *Ifnβ*-luciferase activity, and (D) IBV titres and intracellular RNA
739 were analysed 18 hpi. Bars represent the mean (plus standard deviation) of triplicate wells from a
740 representative experiment. Asterisks indicate significant differences ($P < 0.01$) with respect to the
741 non-RNaseA-treated control (A) or to the siRNA control (B-C), as assessed by one-way ANOVA
742 followed by a Bonferroni post-hoc test.

743

**744 FIG 5. Early accumulation of dsRNA in IBV-infected cells does not result in early
745 induction of *Ifnβ***

746 CEK cells were infected with IBV M41 or IBV Beau-R at the indicated MOIs. At time point 12 hpi (A)
747 dsRNA was visualised in M41-infected cells using an antibody against dsRNA. (B) Expression of *Ifnβ*
748 mRNA was analysed by RT-qPCR. (C) CEK cells were infected with IBV M41 and accumulation of
749 dsRNA was visualised at the indicated time post infection. (D) RNA fluorescent *in situ* hybridisation
750 of *Ifnβ* mRNA in IBV M41-infected CEK cells. Open arrowheads indicate cells that contain dsRNA
751 and no *Ifnβ* mRNA. Solid white arrowheads indicate cells that contain both dsRNA and *Ifnβ* mRNA.

752

**753 FIG 6. Accessory proteins 3a and 3b are involved in regulation of IFN transcription and
754 protein production.**

755 (A) CEK cells were infected with IBV Beau-R 3a/3b (scAUG3ab) or 5a/5b (scAUG5ab) null viruses
756 (MOI 0.1). *Ifnβ* levels were determined using RT-qPCR. (B-D) CEK cells were infected with
757 scAUG3a, scAUG3b or scAUG3ab null IBV viruses (MOI 0.1). In the same cultures (B) *Ifnβ* mRNA,
758 (C) virus titres and (D) type I IFN protein were quantified. Bars represent the mean (plus standard
759 deviation) of triplicate wells from a representative experiment. Significant differences ($P < 0.01$)
760 relative to the Beau-R virus at the same timepoint (*) or between the indicated bars (#) as
761 assessed by a two-way ANOVA followed by a Bonferroni post-hoc test.

762

763 **FIG 7. Signalling of non-self RNA remains intact in IBV-infected cells**

764 (A) CEK cells were infected with IBV M41 for 3 hours and stimulated with extracellular poly I:C (50
765 µg/ml) for an additional 3 hours after which *Ifnβ* transcription was analysed by RT-qPCR. (B) DF-1
766 *Ifnβ*-luc reporter cells were transfected with siRNAs against *Tlr3*, *Mda5* or a control siRNA and 48
767 hours later infected with IPNV (MOI 50); at 6 hpi luciferase activity was quantified. (C) Knockout
768 (KO) and wild-type (wt) MEFs were infected with IPNV (MOI 50) for 8 hours. (D) CEK cells were
769 infected with IBV M41 (MOI 10) for 6h and super-infected with IPNV or UV-inactivated IPNV (MOI
770 50) for an additional 6 h. (E) CEK cells were co-infected with IBV M41 (MOI 5) and RVFV clone 13
771 (MOI 5) and sampled at 6 hpi. (F) DF-1 cells were infected with IBV Beau-R (MOI 1) for 3 h and
772 super-infected with IPNV (MOI 50) or transfected with pI:C (t[pI:C], 500 ng/well) for an additional
773 4 h. (C-F) *Ifnβ* levels were quantified by RT-qPCR. Bars represent the mean (plus standard
774 deviation) of triplicate wells. Significant differences ($P<0.01$) are indicated by (*) as assessed by
775 one-way ANOVA followed by a Bonferroni post-hoc test.

gene	kind	sense	sequence (5'-3')	Accession nr.	reference
TLR3	siRNA	S	UCGAAUACUUGGCUUUA	NM_001011691	
		AS	UUUAAAGCCAAGUUAUCGA		
ctrl	siRNA	S	AGGUAGUGUAAUCGCCUUG	--	
		AS	CAAGGCGAUUACACUACCU		
MDA5	siRNA	S	ACACUGGUAUCAAGUUAUU	GU570144	
		AS	AAUAACUUGAUACCAGUGU		
IFN β	RQ primer	FW	GCTCTCACCACCACCTTCTC	ENSGALT00000039477	
		RV	GCTTGCTTCTTGCTCTTGCT		
IFN α	RQ primer	FW	ATCTGCTGCTCACGCTCTTCT	XM_004937096	40
		RV	GGTGTTGCTGGTGCCAGGATG		
IRF3	RQ primer	FW	CAGTGCTTCCAGCACAAA	NM_205372	
		RV	TGCATGTGGTATTGCTCGAT		
IRF1	RQ primer	FW	CAGGAAGTGGAGGTGGAGAA	ENSGALG00000006785	
		RV	TGGTAGATGTCGTTGGTGCT		
TLR7	RQ primer	FW	TTCTGGCCACAGATGTGACC	NM_001011688	40
		RV	CCTTCAACTTGGCAGTGCGAG		
TLR3	RQ primer	FW	TCAGTACATTTGTAACACCCCGCC	NM_001011691	40
		RV	GGCGTCATAATCAAACACTCC		
MDA5	RQ primer	FW	TGGAGCTGGGCATCTTTCAG	GU570144	
		RV	GTTCCACGACTCTCAATAACAGT		
Mx	RQ primer	FW	TTGTCTGGTGTGCTTCTCT	ENSGALT00000025999	
		RV	GCTGTATTTCTGTGTGCGGTA		
OAS	RQ primer	FW	CACGGCCTCTTCTACGACA	NM_205041	41
		RV	TGGGCCATACGGGTAGACT		
IL8	RQ primer	FW	TTGGAAGCCACTTCAGTCAGAC	NM_205498	41
		RV	GGAGCAGGAGGAATTACCAGTT		
PKR	RQ primer	FW	CCTCTGCTGGCCTTACTGTCA	NM_204487	42
		RV	AAGAGAGGCAGAAGGAATAATTTGCC		
ADAR	RQ primer	FW	TGTTTGTGATGGCTGTTGAG	AF403114	
		RV	AGATGTGAAGTCCGTGTTG		
ISG12	RQ primer	FW	TAAGGGATGGATGGCGAAG	NM_001002856	
		RV	GCAGTATCTTTATTGTTCTCAC		
MHC-I	RQ primer	FW	CTTCATTGCCTTCGACAAAG	NM_001031338	41
		RV	GCCACTCCACGCAGGT		
IFNAR2	RQ primer	FW	GCTTGTGTTTCGTCAGCATT	ENSGALT00000036778	41
		RV	TTCGCAATCTCCAGTTGT		
IBV-N	RQ primer	FW	GAAGAAAACCAAGTCCAGCA	AY851295	
		RV	TTACCAGCAACCCACAC		
Luciferase	RQ primer	FW	TGTTGGGCGGTTATTTATC	X65316	
		RV	AGGCTGCGAAATGTTCACTACT		

Fig.1

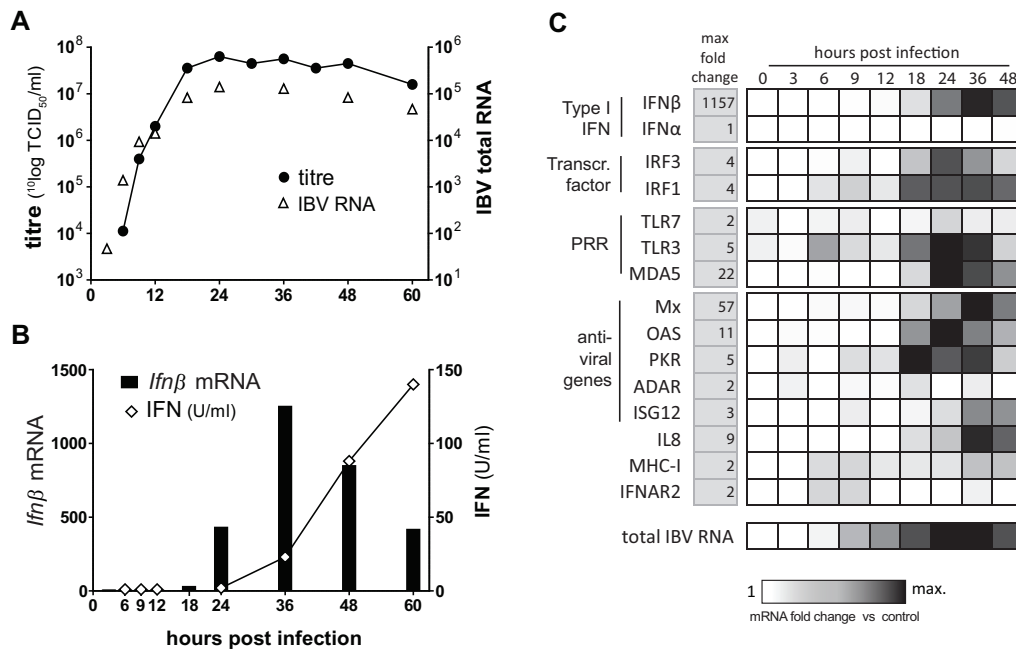


Fig.2

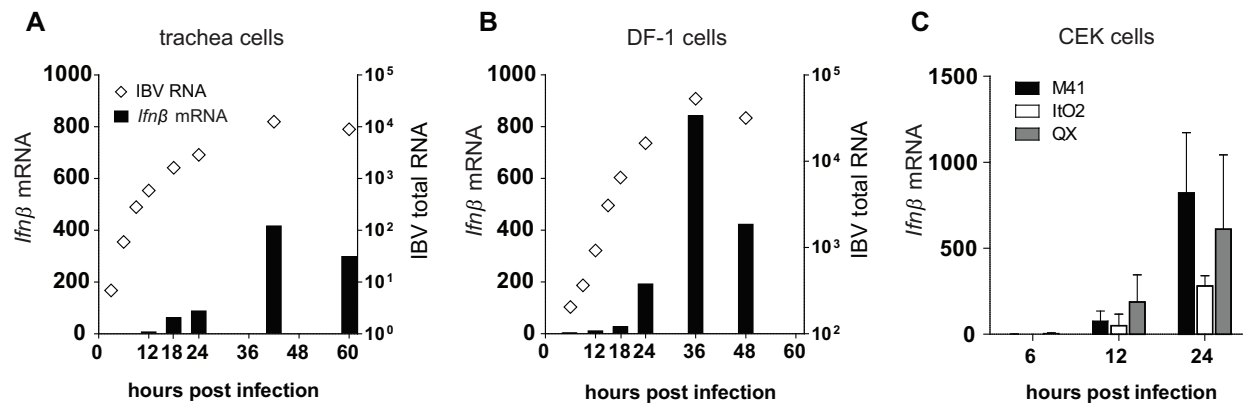


Fig.3

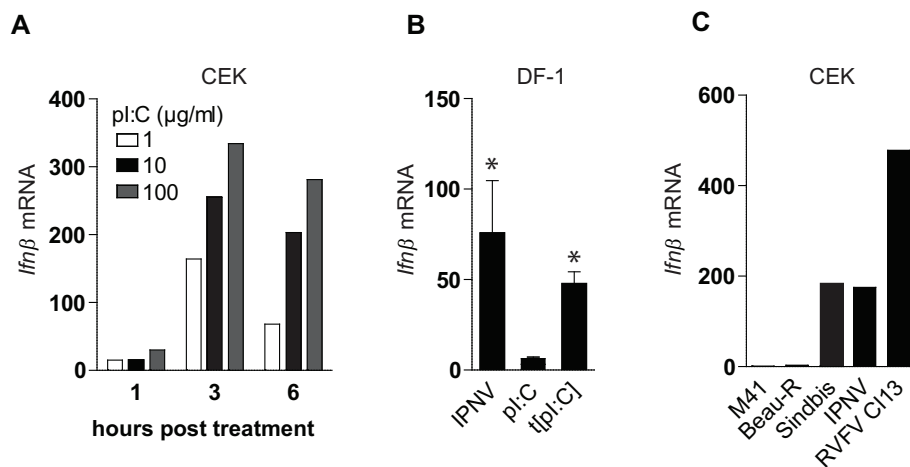


Fig.4

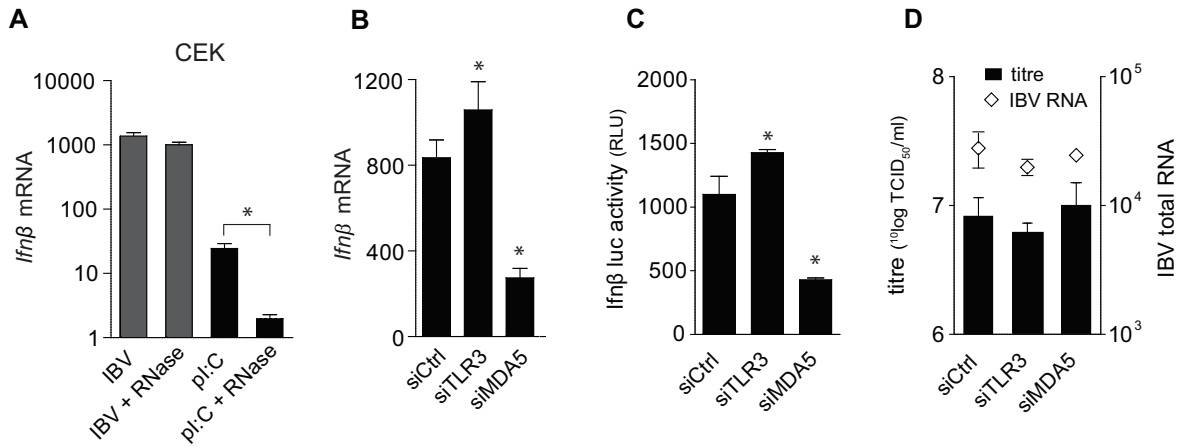


Fig. 5

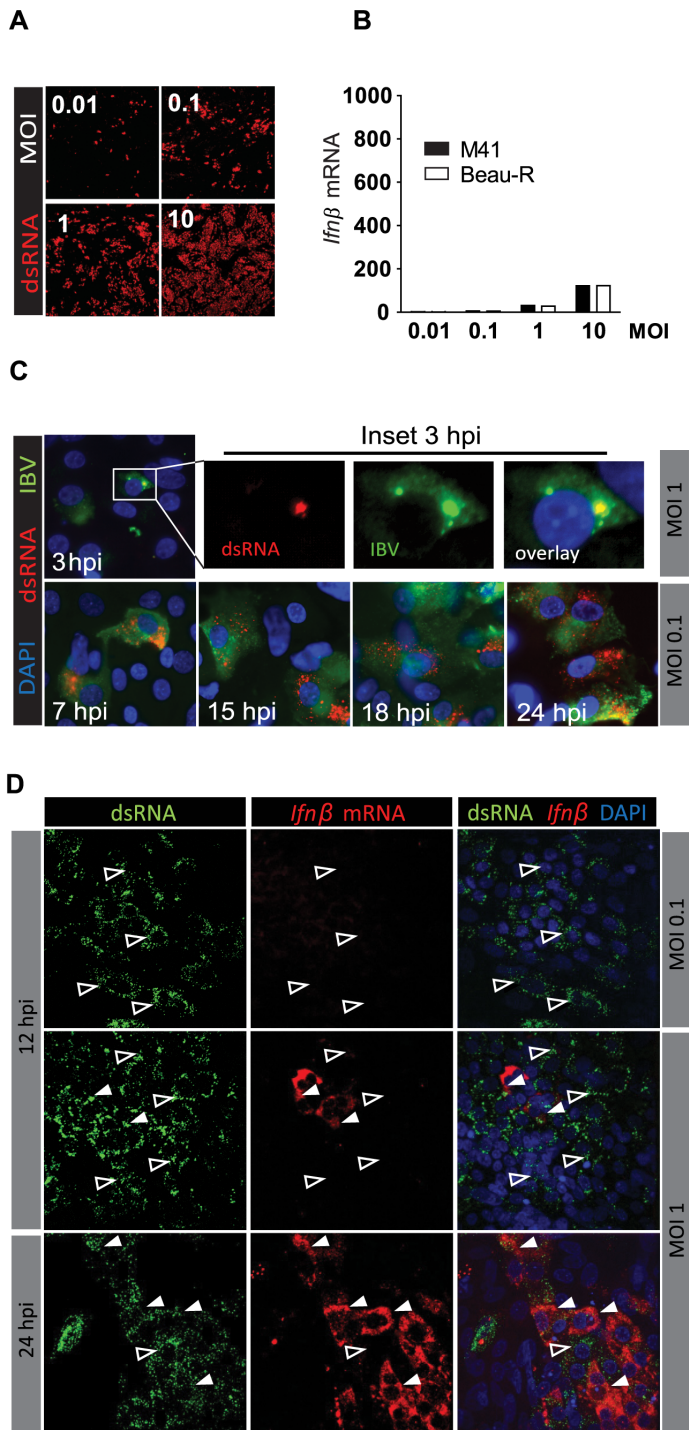


Fig.6

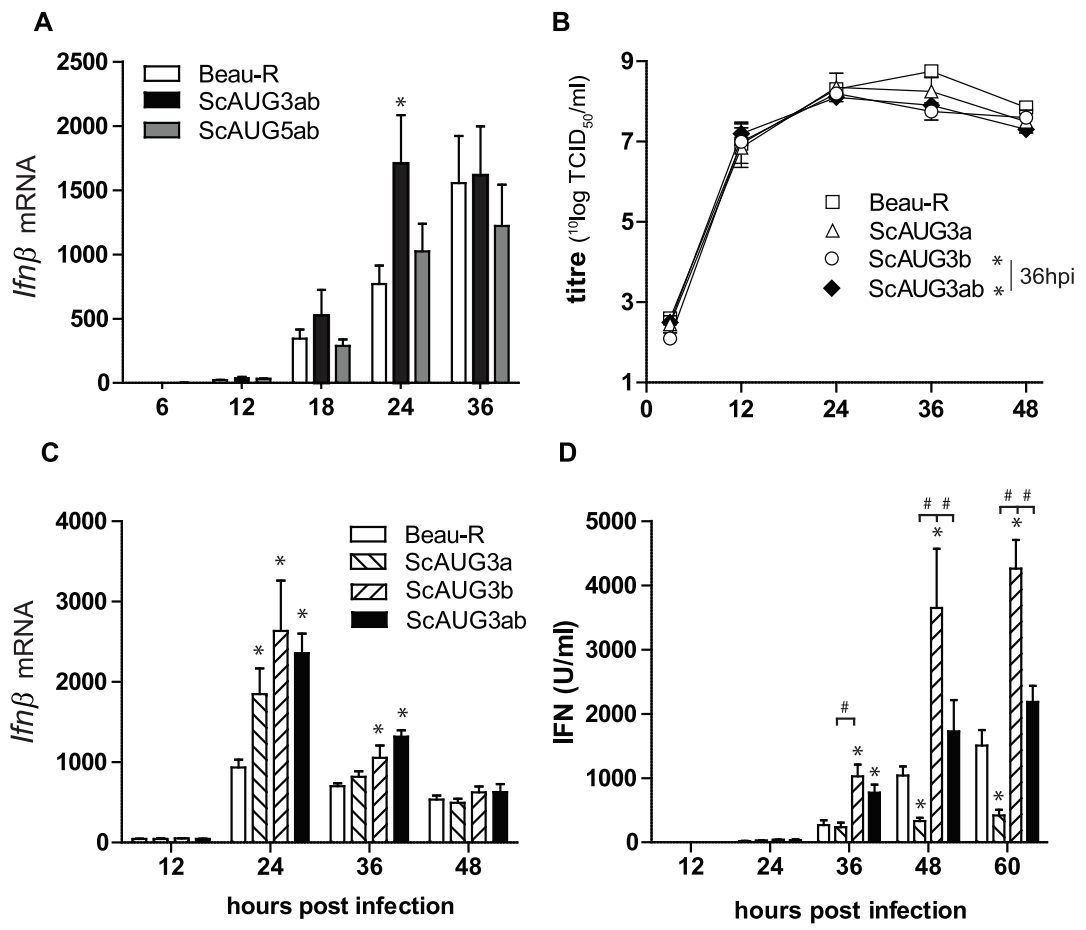


Fig.7

